

Nano-scale thermal transfer

– an invitation to fluctuation electrodynamics

Carsten Henkel^{*†}

^{*} Institute of Physics and Astronomy, University of Potsdam,
Karl-Liebknecht-Str. 24/25, 14476 Potsdam, Germany

Abstract. An electromagnetic theory of thermal radiation is outlined, based on the fluctuation electrodynamics of Rytov and co-workers. We discuss the basic concepts, the status of different approximations. The physical content is illustrated with a few examples on near-field heat transfer.

PACS numbers:

Submitted to: *Zeitschrift für Naturforschung A*, special issue “Heat Transfer and Heat Conduction on the Nanoscale” edited by S.-A. Biehs, P. Ben-Abdallah, and A. Kittel

Introduction

Motivation

The papers in this special issue illustrate that for the management of heat and energy transfer in nano-technology, we are awaiting fundamental challenges. It may suffice to mention Moore’s law according to which on a scale of five to ten years, the microscopic structure of semiconductor junctions will become relevant. We will have to cope with statistical and thermal fluctuations that are significant compared to nominally specified (mean) values. At the same time, it is likely that the design of novel materials with tailored properties in photon and phonon transport opens up new avenues like ‘thermal computing’ and raises the efficiency of thermoelectric and thermo-photovoltaic devices.

† henkel@uni-potsdam.de

In this paper, we intend to provide a gentle introduction into a statistical description of thermal radiation and radiative heat transfer that may guide the engineer from the micro-scale down to the nano-scale. The key tool is already more than 60 years old, it has been dubbed fluctuation electrodynamics and was developed in the 1950s by physicists in the former Soviet Union: Sergei M. Rytov [1], Vladimir L. Ginzburg [2], I. E. Dzyaloshinskii, E. M. Lifshitz, and L. P. Pitaevskii [3,4], just to mention a few. A selection of more recent reviews are Refs. [5–13]. The main idea may be explained by analogy to Brownian motion: instead of characterizing the motion of a particle by its thermal energy, one introduces microscopic trajectories that are perturbed by randomly fluctuating forces. The forces arise from the interaction to a thermal environment, for example between a liquid and a colloidal particle immersed in it. Since the seminal work of Perrin, Langevin and Einstein [14], it has become clear that an ensemble of such fluctuating trajectories can recover (or ‘unravel’) thermal equilibrium statistics and may even describe systems driven out of equilibrium, for example by temperature gradients or external forces.

The radiation field coupled to matter at finite temperature may be described in a similar way. Fluctuation electrodynamics thus takes serious Planck’s idea that thermal equilibrium for blackbody radiation arises from the exchange of energy with the ‘cavity walls’. The latter realize a macroscopic material system whose ‘internal temperature’ imposes the steady state properties of the radiation field. The field is indeed unable to thermalize by itself (excluding extreme situations like the relativistic electron-positron plasma during the first minutes of the Universe). The equations of fluctuation electrodynamics are involving in an essential way the response of the material: dispersion and absorption. It is well known since the 19th century that this can be modelled using material parameters like permittivity, permeability, and conductivity. The main insight of the current trend towards the nano-scale is that this ‘macroscopic description’ can be extended in a quite natural way to scales smaller than the typical wavelengths of thermal radiation (around $1\ \mu\text{m}$, say). There is a relatively large window of scales (the realm of nano-technology) where an atomistic description of matter is not yet needed – it may be dubbed the ‘mesoscopic range’. Let us compute as a rough estimate the ratio between the radiation and matter degrees of freedom. Fixing a cube of size L^3 of a medium with refractive index n , say, the number of photonic modes in a frequency band is

$$\rho_{\text{rad}} d\omega \sim \frac{\omega^2 L^3}{(nc)^3} d\omega, \quad (1)$$

while the microscopic degrees of freedom are given by the atomic number density ϱ/m

$$\rho_{\text{mat}} d\omega \sim \frac{\varrho L^3}{m\omega_D} d\omega. \quad (2)$$

We have assumed for simplicity that the phonon modes are distributed evenly up to the Debye frequency ω_D . Using estimates for a cubic crystal, the photonic mode density is much less by a small factor $\sim (v/c)(a/\lambda)^2 \ll 1$ where v is the speed of sound, a the unit cell size, and λ the photonic wavelength. This illustrates that matter can indeed play the role of a macroscopic reservoir for the radiation field.

For the purposes of this review, we focus on the simplest macroscopic electrodynamics where the material response is assumed to happen locally. Ohm's law, for example, is written $\mathbf{j} = \sigma \mathbf{E}$ where all quantities are evaluated at the same (\mathbf{r}, ω) . In metals, this approximation is expected to work on spatial scales longer than the mean free path of charge carriers and the Fermi wavelength. To the same level of approximation, interfaces between materials are assumed to be 'sharp'. The permittivity $\varepsilon(\mathbf{r}, \omega)$, for example, varies like a step function across the boundary. This is accompanied by suitable boundary conditions for the macroscopic fields. Descriptions that go beyond this picture would use spatial dispersion (non-local response) and genuine response functions for the interface region like a surface current or a surface polarization [15–17]. A discussion of how to formulate fluctuation electrodynamics in nonlocal media can be found in Refs. [18–21].

The last approximation that is commonly applied is the linearity of the medium response. For material parameters like ε , linear response is written into its definition. The physics beyond this regime is very rich and contains effects like rectification of thermal noise, generation of higher harmonics, temperature-dependent material parameters, hysteresis, and so on. Some of these aspects are already studied in nano-scale thermal devices, in the proposals for thermal diodes or rectifiers, for example. Others are being explored theoretically [22, 23]. From a mathematical viewpoint, the linear approximation provides a simple link between the probability distributions of the Langevin forces (matter-related sources of the field) and of the field, yielding eventually to Gaussian statistics which is completely characterized by mean values and the correlation spectra.

A number of recent experiments on nano-scale heat transfer can be found in this Special Issue, one of the oldest we are aware of is from the Dransfeld group [24]. We shall comment on a few recent references in this paper. As a side remark, we

mention techniques where thermal dynamics becomes accessible on short time scales, comparable to the equilibration time between electron and phonons [25]. They may provide a complementary approach to a better understanding of heat transport, where the transient response of matter is in the focus.

The sketch in Fig.1 below is meant to fix some ideas: two bodies are described as extended objects with sharp boundaries. Inside, a local temperature can be defined, although its variation may be weak despite a sizeable heat current. The bodies are separated by a vacuum gap across which photons are ‘propagating’ and ‘tunnelling’ to transport energy. Direct contact which would lead to phononic and electronic transport, can be excluded by working at distances above a few Ångstrom.

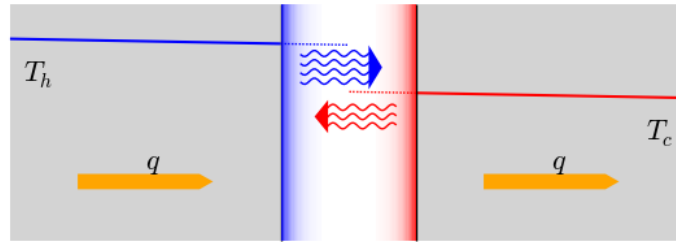


Figure 1. Typical setting of a heat transfer experiment on the nano-scale. The blue and red lines give the temperature profile in the two bodies (left: hot, right: cold). The heat current q is carried by conduction in the body and by the difference of thermal emission in the gap. The blue and red shadings illustrate the evanescent waves in the near-field of the surfaces; they provide additional ‘tunnelling channels’ for heat transfer. This can lead to an amplification by a few orders of magnitude above the Stefan–Boltzmann law.

Rytov formulation of fluctuation electrodynamics

Maxwell-Langevin equations

Within the approximations outlined in the Introduction, the radiation field in a mesoscopic medium is described by the following set of macroscopic Maxwell equations

$$\begin{aligned} \nabla \cdot \varepsilon \mathbf{E} &= \rho, & \nabla \times \mathbf{H} - i\omega \varepsilon \mathbf{E} &= \mathbf{j} \\ \nabla \cdot \mu \mathbf{H} &= 0, & \nabla \times \mathbf{E} - i\omega \mu \mathbf{H} &= \mathbf{0} \end{aligned} \quad (3)$$

Here, $\varepsilon = \varepsilon(\mathbf{r}, \omega)$ and μ describe the electric and magnetic response of the medium. The charge and current densities can be represented by ('external') polarization and magnetization fields

$$\rho = -\nabla \cdot \mathbf{P}, \quad \mathbf{j} = -i\omega\mathbf{P} + \nabla \times \mathbf{M} \quad (4)$$

In the case of non-magnetic and local conductors, the key response function is the conductivity σ , and Eqs.(3) apply with $\varepsilon = \varepsilon_0 - i\sigma/\omega$, $\mu = \mu_0$, and $\mathbf{M} = \mathbf{0}$. In some applications to thermal radiation in metals, a 'background' dielectric response (due to the ionic cores) is taken into account, replacing ε_0 by ε_b inside the conductor.

The boundary conditions for the fields at a smooth interface follow from the Maxwell equations (3) when understood in the sense of distribution theory: a jump in the normal component of the displacement field $\varepsilon\mathbf{E}$, for example, is given by the surface charge density, i.e., a δ -sheet of $\rho(\mathbf{r})$, localized at the interface. Similar techniques may be applied when the response functions vary rapidly near the interface on the spatial scales relevant for the fields. One may introduce a 'macroscopic' model for the interface where the material equations are extrapolated from the two bulk media to the surface. The deviations from this extrapolation are called 'excess charges' or currents and are represented by δ -distributions localized on the (macroscopic, idealized) interface. For details, see the books [15,16].

The key idea of fluctuation electrodynamics, developed by Rytov and co-workers [1], is that the sources ρ, \mathbf{j} are random or fluctuating fields. This is why we shall call Eqs.(3) the Maxwell-Langevin equations. If the sources are nonzero on average, their values would be interpreted as 'external' charges as in the conventional macroscopic electrodynamics. The fluctuations around the average arise from the thermal motion of carriers in the medium and are therefore determined by its temperature and its 'oscillator strength' (or density of states). Within the macroscopic scheme, as explained above, it is natural to apply local thermodynamic equilibrium statistics to describe the charge and current fluctuations.

Source (current) fluctuations

To illustrate these concepts, let us take as an example the current fluctuations in a conductor and assume for simplicity that the mean value $\langle \mathbf{j}(\mathbf{r}, \omega) \rangle = \mathbf{0}$. The fluctuations of the current define its noise spectrum as follows

$$\langle j_m^*(\mathbf{r}', \omega') j_n(\mathbf{r}, \omega) \rangle = 2\pi\delta(\omega' - \omega) \langle j_m(\mathbf{r}') j_n(\mathbf{r}) \rangle_\omega \quad (5)$$

The writing $\langle \dots \rangle_\omega$ on the rhs is adopted to avoid additional notation, although it is, strictly speaking, slightly abusive. This quantity provides the (power) spectral density, i.e. the Fourier transform of the autocorrelation function (Wiener-Khintchin formula)

$$\langle j_m(\mathbf{r}', t') j_n(\mathbf{r}, t) \rangle = \int_{-\infty}^{\infty} \frac{d\omega}{2\pi} e^{i\omega(t'-t)} \langle j_m(\mathbf{r}') j_n(\mathbf{r}) \rangle_\omega \quad (6)$$

Note that the factor 2π in Eq.(5) is tied to this convention for the Fourier transform and that such a definition makes sense in a stationary situation only (correlations only depend on the time difference). The complex Fourier expansion used here is appropriate for ‘quantum detectors’ like a photomultiplier. Glauber’s theory of these detectors works with the hermitean field operator $\mathbf{E}(\mathbf{r}, t)$ and shows that the signal involves the convolution of \mathbf{E} with a complex exponential $e^{-i\omega t}$ where $\omega > 0$ is the threshold frequency (work function). In classical electronics, the signal is convolved with a real-valued reference or circuit response. In that case, an autocorrelation function based on a symmetrized operator product is relevant. Its spectrum is symmetric and is equal to the average of its ‘quantum cousin’ (6) over positive and negative frequencies.

Thermal equilibrium and local macroscopic electrodynamics yield the following relation between spectrum and conductivity

$$\langle j_m(\mathbf{r}') j_n(\mathbf{r}) \rangle_\omega = 2\hbar \frac{\omega \operatorname{Re} \sigma(\omega)}{e^{\hbar\omega/k_B T} - 1} \delta_{mn} \delta(\mathbf{r}' - \mathbf{r}) \equiv S_j(\mathbf{r}, \omega) \delta_{mn} \delta(\mathbf{r}' - \mathbf{r}) \quad (7)$$

where both $T = T(\mathbf{r})$ and σ may vary spatially (local temperature). The real part (the conductance) of the complex admittance σ is related to Ohmic dissipation, hence the name fluctuation–dissipation (FD) relation for Eq.(7). This formula is the quantum extension of Johnson–Nyquist noise, see the seminal paper by Callen and Welton on the FD theorem [26] and the review by Ginzburg [2]. The current spectrum $S_j(\mathbf{r}, \omega)$ is plotted in Fig.2 inside a Drude conductor, $\sigma(\omega) = \sigma_{\text{DC}}/(1 + i\omega\tau)$. The plot covers both positive and negative frequencies: note the asymmetry of the spectrum. This is typical for operator products that are not in symmetric order and hence a typical quantum effect. Indeed, with our convention for the spectral density, quantum (or vacuum) fluctuations become visible at negative frequencies. The scheme required to detection these would be based not on absorption, but on emission (spontaneous and stimulated), see for example Ref. [27]. The quantum current fluctuations in a Drude conductor show a broad Debye-like peak at $\omega \sim -1/\tau$ where τ is the electronic relaxation time. (The mean free path is $v_F\tau$ with v_F the Fermi

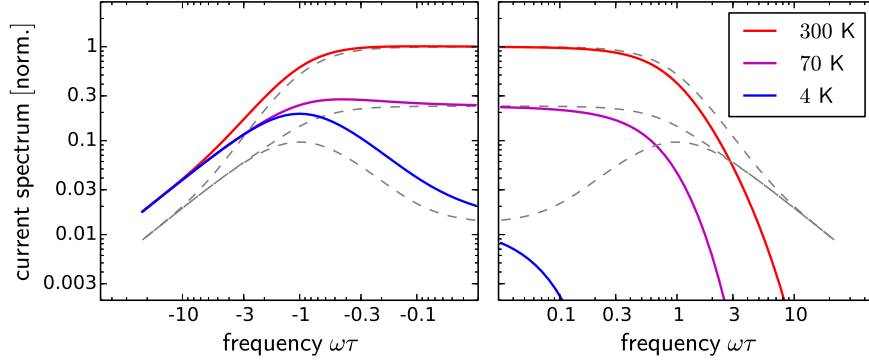


Figure 2. Spectral density $S_j(\omega)$ of current fluctuations inside a Drude conductor, Eq.(7), for positive and negative frequencies. The spectrum is normalized to its low-frequency limit at $T = 300$ K [see Eq.(8)], the temperature dependence of σ_{DC} is neglected for simplicity. The frequency is normalized to the Drude relaxation rate $1/\tau$ (we took $\hbar/\tau = 10$ meV). The dashed lines give the spectrum for the symmetrized autocorrelation of the current.

velocity.) Another convention is to take a symmetrized correlation function so that the spectrum becomes symmetric (gray dashed lines).

At lower frequencies, the current noise is white and given by the Nyquist formula,

$$\langle j_m(\mathbf{r}') j_n(\mathbf{r}) \rangle_\omega \approx 2k_B T \sigma_{\text{DC}} \delta_{mn} \delta(\mathbf{r}' - \mathbf{r}) \quad (8)$$

It is interesting to note that for typical Drude parameters and room temperature, the ‘thermal energy-time uncertainty product’, $k_B T \tau / \hbar$, is not far from unity. In other words, good conductors show strongly damped electrical currents at room temperature.

Field correlations

The thermal radiation field generated by the Rytov-Langevin Eqs.(3) depends linearly on its sources. Solutions to the homogeneous equations can be used to describe radiation incident from infinity [28]. Some authors prefer to cancel these solutions by allowing for a nonzero imaginary part in $\varepsilon(\mathbf{r}, \omega)$ in all space (see, for example, Ref. [29]). We follow this route and get for bodies in local equilibrium the following expression for the electric field correlation function (defined as in Eq.(5),

summation over double indices):

$$\langle E_k(\mathbf{r}) E_l(\mathbf{r}') \rangle_\omega = \int d^3s G_{km}^*(\mathbf{r}, \mathbf{s}, \omega) G_{lm}(\mathbf{r}', \mathbf{s}, \omega) S_j(\mathbf{s}, \omega) \quad (9)$$

Here $G_{kl}(\mathbf{r}, \mathbf{s}, \omega)$ is the electromagnetic Green tensor which gives the electric and magnetic fields radiated by a point current source located at \mathbf{s} :

$$E_k(\mathbf{r}, \omega) = \int d^3s G_{kl}(\mathbf{r}, \mathbf{s}, \omega) j_l(\mathbf{s}, \omega) \quad (10)$$

$$H_k(\mathbf{r}, \omega) = \frac{-i}{\omega \mu(\mathbf{r}, \omega)} \epsilon_{klm} \frac{\partial}{\partial r_l} \int d^3s G_{mn}(\mathbf{r}, \mathbf{s}, \omega) j_n(\mathbf{s}, \omega) \quad (11)$$

As a function of \mathbf{r} and the index k , G_{kl} satisfies the boundary conditions at macroscopic interfaces. Many different conventions for prefactors in Eqs.(10, 11) appear in the literature. Explicit expressions are available in free space [30], at a planar interface [31, 32] and in multi-layer structures [33], in spherical [34] and cylindrical geometries [35]. The book by Chew [36] provides an exhaustive discussion, including numerical techniques from computational electrodynamics. Let us simply note that in practice, it is possible to avoid the volume integration in Eq.(9) and get instead an integral over the surfaces of the bodies [9, 37, 38]. (The price to pay is the restriction to spatially constant temperatures inside the bodies.) For objects with highly symmetric shape, an expansion into orthogonal vector field modes is possible ('principle of sufficient symmetry'), reducing Eq.(9) to a summation over products of mode functions.

From a correlation function like $\langle E_k(\mathbf{r}) E_l(\mathbf{r}') \rangle_\omega$, it is easy to compute the electromagnetic energy density (take $k = l$ and $\mathbf{r} = \mathbf{r}'$), correlations for the magnetic field (take the curl with respect to both \mathbf{r} and \mathbf{r}'), and the Poynting vector, for example. All quantities naturally appear in the spectral domain, and can be split into contributions originating from the different objects. In this way, heat currents from body A to B and back can be determined by computing the flux of the Poynting vector across a surface that separates A and B [see Eq.(20) below]. The elements of the electromagnetic stress tensor [30], plotted locally, permit to visualize forces (momentum transfer) between objects, providing physical insight into dispersion and Casimir forces; see Ref. [39] for examples. A seminal example of this problem is Lifshitz' derivation of the van der Waals force between macroscopic bodies [3, 40].

Quantum field theory

The Maxwell-Langevin approach sketched so far provides the equations of motion of the field (operators), and relevant averages (correlation functions) are obtained

from those of the source currents. The question has been raised what would be the Hamiltonian of this theory. The quantization scheme for the macroscopic Maxwell equations developed by the Knöll and Welsch group in Jena [29,41] gives an answer in line with the ideas of Rytov and co-workers [1]: the information contained in the macroscopic medium response functions (dielectric function ε, \dots) is sufficient. We adopt here a slight re-writing of the Jena equations and keep working with the current operators $\mathbf{j}(\mathbf{r}, \omega)$. The basic idea is to upgrade each Fourier component to a dynamic variable. The medium+field Hamiltonian is then given by the sources alone

$$H_{\text{MF}} = \int_0^\infty \frac{d\omega}{2\pi} \int d^3r \frac{\mathbf{j}^*(\mathbf{r}, \omega) \cdot \mathbf{j}(\mathbf{r}, \omega)}{2 \operatorname{Re} \sigma(\omega)} \quad (12)$$

It is interesting that the power density of Joule absorption provides the energy (12) of medium and field. The Heisenberg equations of motion yield the seemingly trivial time evolution $\sim e^{-i\omega t}$ provided the commutator of the currents is chosen as

$$[j_m(\mathbf{r}', \omega'), j_n^*(\mathbf{r}, \omega)] = 4\pi\hbar\omega \operatorname{Re} \sigma(\omega) \delta_{mn} \delta(\mathbf{r}' - \mathbf{r}) \delta(\omega' - \omega) \quad (13)$$

The relation $\mathbf{j}(\mathbf{r}, \omega) = \mathbf{j}^*(\mathbf{r}, -\omega)$ is imposed as initial condition and is preserved during the evolution. The local thermal equilibrium ensemble is generated by a density operator proportional to the exponential of H_{MF} , taking the local temperature field $T(\mathbf{r})$ under the spatial integral in Eq.(12). The FD relation with its correlation function (7) then follows.

The observable electric field is given by the source current convolved with the Green function [Eq.(10)], and this relation can be understood as a generalized mode expansion. In this way, the Maxwell-Langevin equations are satisfied. The coupling to external sources (atoms or molecules) proceeds in the usual way by adding interaction terms to H_{MF} . A multipolar coupling scheme is quite natural, for details see the book by Buhmann [41]. An important consistency check is to recover the Pauli-Jordan commutator between the electric and magnetic fields:

$$[E_i(\mathbf{r}, t), B_j(\mathbf{r}', t)] = -\frac{i\hbar}{\varepsilon_0} \epsilon_{ijk} \frac{\partial}{\partial x_k} \delta(\mathbf{r} - \mathbf{r}') \quad (14)$$

This is achieved by using Eq.(13) for the source currents, the Kramers-Kronig relations for the Green function, and the following identity [42,43]

$$\int d^3s \operatorname{Re}(\sigma) G_{ik}^*(\mathbf{r}, \mathbf{s}) G_{jk}(\mathbf{r}', \mathbf{s}) = -\operatorname{Re} G_{ij}(\mathbf{r}, \mathbf{r}') \quad (15)$$

that follows from the classical macroscopic Maxwell equations. The frequency arguments were suppressed for simplicity, and the negative real part appearing on

the rhs is due to the convention adopted here for the Green tensor [compare to the energy conservation law (19) below].

Discussion

Let us finish this basic introduction with a remark on physical interpretation. A cursory scan through the literature yields different answers as to the actual status of the current fluctuations appearing in Eqs.(3, 7). One may consider them as *mathematical artefacts* whose only merit is to reproduce, in thermal equilibrium, the spectrum of the radiation field [44], similar to thermostatting Langevin forces in molecular dynamics. It has been checked that equilibrium is indeed recovered if all bodies are at the same temperature: the field then follows Planck's blackbody spectrum, modified by the bodies' emissivity and enhanced significantly when near-field components become detectable at sub-wavelength distances [44]. Right from its inception, however, fluctuation electrodynamics has been applied to non-equilibrium settings, too [4], where this reference situation is no longer available. One is then inclined to adopt the viewpoint that Rytov's fluctuating currents are a model for *actual thermal fluctuations* of matter observables that are relevant as electromagnetic sources—an approximate model, of course, since in the formulation presented above, the local macroscopic theory has been applied. But the model has some reasonable footing given the large number of microscopic constituents that make up a condensed-matter system on a mesoscopic length scale of, say, a few nanometers [see Eq.(2)]. The key assumption is, of course, that on this scale, the concept of a local temperature $T(\mathbf{r})$ makes sense, and that the electromagnetically relevant quantities have fluctuations that are equilibrated at this temperature. Such a model is eventually required in any description, as described insightfully by Barton [45]:

One could of course try to pursue the further question how the Langevin forces themselves might be kept functioning as envisaged; to explore this would then entail hypothesising some thermostats controlling the forces, and calculating the forces instead of making assumptions about them a priori; and so on, potentially ad infinitum. In the end, one must necessarily settle for control at some level through thermostats that are external to the system, in the sense that they impose temperatures by fiat, through dynamics that do not enter the calculation and are not spelled out.

The following formula may illustrate the problem of local equilibrium

$$\mathbf{j}_{\text{tot}}(\mathbf{r}, \omega) = \sigma \mathbf{E}(\mathbf{r}, \omega) + \mathbf{j}(\mathbf{r}, \omega) \quad (16)$$

This sum (sometimes called the ‘Rytov split’) gives the current as the sum of Ohm’s law (‘induced current’), while the second term gives the fluctuations around this value (‘fluctuating current’, sometimes marked with subscript fl). In a non-equilibrium setting like in heat transfer, the field $\mathbf{E}(\mathbf{r}, \omega)$ is in general not in a state of local equilibrium because it contains radiation from distant sources at different temperatures. The current is then not in local equilibrium neither, because its induced part is simply the linear (and local) response of the medium to this non-equilibrium field. But the fluctuations around it (fluctuating current) are characterized by the local temperature. This has been recognized as the key assumption of fluctuation electrodynamics, for example by Barton [45,46] who comments in Ref. [45] on Loomis and Maris [47]:

[...] who do not assume local thermal equilibrium, but only that in each half-space the noise is appropriate to the temperature of its thermostat.

It is, of course, another problem how local thermal equilibrium is established in the material, and whether this happens fast enough to talk of a single temperature for all frequencies of the local current noise. A practically-minded engineer might want to use an equation of motion for the temperature distribution $T(\mathbf{r})$ using a combination of heat conduction and heating/cooling by absorption/emission of thermal radiation. It seems quite obvious that such a ‘self-consistent’ model requires a separation of time scales between the ‘fast’ electromagnetic fluctuations and the ‘slow’ evolution of the temperature field. Needless to say that for many experiments on near-field radiative transfer, it is sufficient to assume a stationary temperature profile, which may even be spatially flat (across each body) if the thermal conductivity is large enough. For a counter-example on short time scales, see the experiment of the Bargheer group quoted above [25].

As a quick estimate, let us consider a typical nano-scale heat flux that aims at competing with the solar constant, $q = 1360 \text{ W/m}^2$. Typical thermal conductivities of condensed matter are in the range $\kappa = 1 \dots 10^2 \text{ W/K m}$ at room temperature. On the spatial scale L of a microdevice, one thus estimates a temperature difference

$$\Delta T \sim L \frac{\Delta T}{L} \sim L \frac{q}{\kappa} \sim 10^{-5} \dots 10^{-3} \text{ K} \times (L/1 \mu\text{m}) \quad (17)$$

which is probably below the precision of typical thermometry. In a nano-junction, the temperature profile is thus ‘step-like’ (see Fig.1). The radiation field in the gap

between the bodies has no well-defined temperature, of course. This is similar to radiation in the upper atmosphere which is a superposition of solar and terrestrial sources.

Examples

We now present a few examples of results from fluctuation electrodynamics. Two viewpoints will be stressed: the differences to radiative transfer which describes thermal radiation on larger scales [48], and challenges beyond the mesoscopic theory presented so far.

Typical features on the nano-scale

Thermal radiation is a classical topic in astrophysics where it determines the luminosity and the inner structure of stars. The cosmic microwave background also provides an example where the blackbody spectrum is a very accurate description.

As one works with condensed matter sources, deviations from the Planck spectrum become apparent. Some of these are well-known and are described by the classical Kirchhoff concepts of emissivity and absorption ('grey bodies') [48]. As one enters the near field, the changes in the spectrum become dramatic because surface resonances may appear in the range of thermal frequencies. Polar materials provide a generic example where optical phonons hybridize with the electromagnetic field into surface phonon polaritons. These resonances enhance the electromagnetic energy density and they also polarize the radiation field. An example is shown in Fig.3 for a planar body: at the wavelength $11.36 \mu\text{m}$, silicon carbide has surface resonances (because the permittivity is negative) which show up as a prominent 'shoulder' at distances $d \approx \lambda/10$. At even shorter distances, the energy density follows a law $1/d^2$ which can be explained by the electrostatic fields of fluctuating dipole moments. The surface resonance appears as an enhanced amplitude of this power tail.

The polarization of the near field has been quantified in the plot by the following degree of polarization[‡]

$$P = \frac{|\varepsilon_{\parallel} - \varepsilon_{zz}|}{\varepsilon_{zz} + 2\varepsilon_{\parallel}}, \quad 0 \leq P \leq 1 \quad (18)$$

[‡] Eq.(18) arises from Refs. [49,50] which coincide in the present situation. They do not so in the general case, because of different ways the three field components have been taken into account to define degrees of polarization. For a comparison, see Ref. [11].

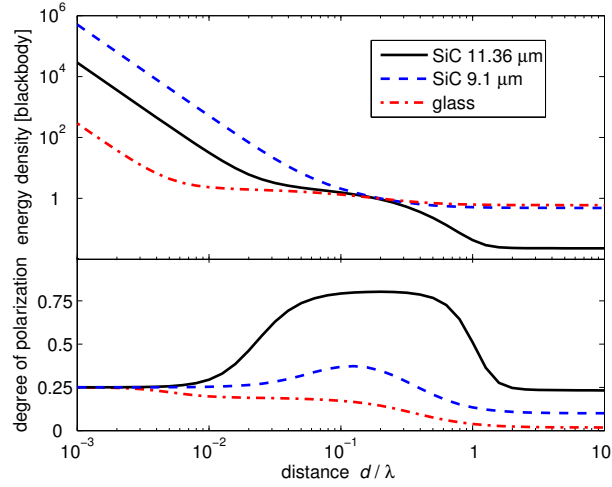


Figure 3. Electric energy density spectrum as a function of distance (top panel) and degree of polarization (bottom panel). Parameters for SiC: $\varepsilon(11.36 \mu\text{m}) = -7.6 + 0.4i$ and $\varepsilon(9.1 \mu\text{m}) = 1.8 + 4.0i$; for glass $\varepsilon(500 \text{ nm}) = 2.25 + 10^{-3}i$. The energy densities follow a power law $1/d^2$ at short distances. They have been normalized to the Planck spectrum. Figure adapted from Ref. [11], Fig. 8.

where ε_{zz} (ε_{\parallel}) is proportional to the spectrum of the electric field perpendicular (parallel) to the surface and by symmetry, $\langle E_x^2(\mathbf{r}) \rangle_{\omega} = \langle E_y^2(\mathbf{r}) \rangle_{\omega}$. Note the strong polarization when the surface resonance is excited. In the limits of short and large distances, a partial polarization $P \approx 1/4$ arises, but for different reasons: at short distances, it follows from electrostatics that the normal field (E_z) has a spectrum twice as large as the parallel field. At large distances, the polarization is due to reflection and emission at glancing angles from the surface, similar to the Brewster effect. This partial polarization is actually an artefact of assuming a planar source of infinite extent. For a discussion of the thermal emission of a spherical source, see for example Refs. [51, 52].

Let us mention that to measure the energy density, a local measurement with a small pick-up antenna is needed. This can be achieved with sharp tips that scatter the near field [53], see the contribution of De Wilde in this issue. The scattered signal is dominated by the immediate environment of the local probe: a lateral resolution comparable to the distance d would be typical. In this way, the thermal radiation may provide a scanning image of local electromagnetic properties and resolve metallic nano-objects on a dielectric substrate, for example.

Energy balance and radiative heat transfer

The radiative heat flux between two objects is described in electromagnetism by the Poynting vector. In our context, it has a natural spectral representation and involves the Planck spectrum as an essential factor, due to the assumption of local thermal equilibrium of the radiation sources. The symmetry of photons propagating to the left and the right is broken by the difference in temperature. As the bodies are approached to sub-wavelength distances, the heat flux is enhanced due to near-field coupling.

Let us start with the energy conservation law for the Maxwell-Langevin equations. In a stationary situation (the energy density is constant), one gets

$$\nabla \cdot \text{Re}\langle \mathbf{E} \times \mathbf{H} \rangle_\omega + \omega \text{Im} \varepsilon(\omega) \langle \mathbf{E}^2 \rangle_\omega = -\text{Re}\langle \mathbf{j} \cdot \mathbf{E} \rangle_\omega \quad (19)$$

for each frequency ω . The first term on the lhs involves the radiative emission spectrum (average Poynting vector $\langle \mathbf{S} \rangle_\omega$), the second term the absorption in the medium. (With our sign convention, passive media have $\omega \text{Im} \varepsilon(\omega) \geq 0$.) On the rhs, we find the power transferred to the fields by the mechanical motion of the sources [30]. Eq.(19) has been commented upon in a discussion of energy conservation in a dissipative system [54]: the electromagnetic energy lost by absorption in the medium is ‘replenished’ by the sources in the same medium, as long as local equilibrium holds. This observation illustrates the general idea of treating dissipative quantum systems with Langevin dynamics: the fluctuating forces maintain the system energy at its equilibrium value. By the same token, they prevent the commutators of the system observables from decaying.

In a typical setting of heat transfer between two bodies, we may evaluate Eq.(19) in a vacuum gap between them and get $\nabla \cdot \langle \mathbf{S} \rangle_\omega = 0$. In a planar geometry, this means that the normal flux is constant. We quote here the formula that results from evaluating the mixed electric and magnetic correlation function between two planar bodies, ‘hot’ and ‘cold’, at distance d [47,55]

$$\langle S_z \rangle_\omega = [\Phi(\omega, T_h) - \Phi(\omega, T_c)] \sum_p \int \frac{k \, dk}{(\omega/c)^2} A_{hp} A_{cp} \left| \frac{e^{2ik_z d}}{1 - r_{hp} r_{cp} e^{2ik_z d}} \right|^2 \quad (20)$$

$$\Phi(\omega, T) = \frac{\hbar \omega^3}{4\pi^3 c^2} \frac{1}{e^{\hbar \omega / k_B T} - 1} \quad (21)$$

where $\Phi(\omega, T)$ is the flux of a black body. Two polarizations p are summed over, and

the quantity

$$0 \leq A_{bp} = \begin{cases} 1 - |r_{bp}|^2 & \text{if } k \leq \omega/c \\ 2 \operatorname{Im} r_{bp} & \text{if } k > \omega/c \end{cases} \quad (22)$$

is proportional to the absorption of a wave incident on body $b = h, c$ where it is reflected with amplitude $r_{bp} = r_{bp}(k, \omega)$. Finally, $k_z = \sqrt{(\omega/c)^2 - k^2}$ is the normal component of the wavevector in vacuum. For $k > \omega/c$, it is purely imaginary (evanescent wave, $\operatorname{Im} k_z \geq 0$), the heat then transports by photon tunnelling from the bulk of one body to the other. The denominator $1 - r_{hp}r_{cp} e^{2ik_z d}$ in Eq.(20) describes the multiple reflection of waves between the two interfaces; its zeros correspond to ‘cavity modes’ and surface resonances. In practice, due to imperfect reflections, the modes are broadened but are still visible in the spectrum. See Fig.4 for an example, taken from the seminal paper by Polder and Van Hove [55].

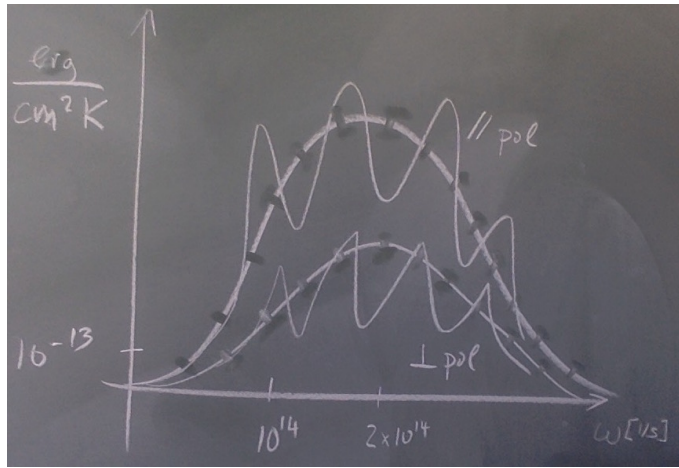


Figure 4. Spectrum of heat flux between two metallic slabs, contribution of propagating waves ($0 \leq k \leq \omega/c$ in Eq.(20)). Upper pair of curves: electric field in the plane of incidence (p- or TM-polarization), lower pair: electric field perpendicular to plane of incidence (s or TE). Solid lines: distance $d = 10 \mu\text{m}$, dashed lines: $d \rightarrow \infty$. The peaks arise when d is an integer multiple of $\lambda/2$ (standing waves). The bodies are at temperatures $T_h = 315 \text{ K} = T_c + 1 \text{ K}$, and have identical conductivities described by a Drude model with $\sigma_{\text{DC}} = 3.9 \text{ MS/m}$ and damping time $\tau = 7.1 \text{ fs}$. Sketch after Fig. 4 of Ref. [55]: D. Polder and M. van Hove, “Theory of radiative heat transfer between closely spaced bodies”, *Phys. Rev. B* **4** (1971) 3303.

The enhancement of the heat flux in the near field is mainly due to the contribution of evanescent waves (photon tunnelling). Taking the limit of purely non-absorbing bodies, one finds that the k -integral in Eq.(20) is limited to $k \leq$

$n\omega/c$ where n is the refractive index: in this case, the Planck spectrum (Stefan-Boltzmann law) still holds with a modified prefactor (angle-averaged emissivity). Fig. 4 illustrates that the propagating modes that dominate in this range mainly redistribute the emission spectrum by forming cavity resonances. The qualitatively new power laws seen in Fig.3 emerge from deeply evanescent waves, $k \gg \omega/c$. These correspond, on one hand, to surface polaritons with typically $k \sim 1/d$ where d is the distance, and on the other, to diffusion ‘modes’, $k \sim (\mu_0\sigma_{\text{DC}}\omega)^{1/2}$, where $(\mu_0\sigma_{\text{DC}})^{-1}$ is the magnetic diffusion constant in a conductor. From an analysis of the two polarizations, these contributions have been pointed out already by Polder and Van Hove [55].

Challenges

For recent applications of fluctuation electrodynamics, see other papers in this issue. We conclude this discussion with two challenges that may lead to a refined theory. By analogy to the unexplained perihelion shift of Mercury about hundred years ago, we suggest to name the following observations ‘anomalies’.

Casimir force and conductivity

The first anomaly has been dubbed the ‘plasma vs. Drude controversy’ in the community working on dispersion forces and the Casimir effect [56,57]. We focus here on an experiment, performed by the Mohideen group [58], that does not seem to have received much attention in this discussion. In the setup, an atomic force microscope is measuring the force between a sphere (diameter $\sim 200 \mu\text{m}$) and a planar body. The body is a semiconductor membrane (silicon) and gets irradiated with a train of laser pulses that increases the carrier density. The density is practically stationary over the $\sim 5 \text{ ms}$ duration of the pulses, and the force is measured with a lock-in amplifier at the repetition rate. From the viewpoint of macroscopic electrodynamics, the irradiation changes the conductivity by a few orders of magnitude from quite small (intrinsic, related to defects, $\sim 10 \text{ S/m}$) to high ($\sim 1 \text{ MS/m}$), while the temperature increase is negligible.

The calculated change in the electromagnetic force agrees with the experimental data within 10%, but only for the laser-doped material. A statistically significant difference to the theory (about 50% at distance $d \approx 100 \text{ nm}$) is observed for the intrinsic Si membrane. The deviation can be pinpointed to the behaviour of the

material conductivity across the thermal spectrum (see Refs. [59,60] for a discussion). Technically speaking, frequency integrals are performed as summations over the imaginary axis (Matsubara sum), using the analytical continuation of response functions. The anomaly arises from the zero-frequency term in the sum. The current discussion about this thermal Casimir anomaly has led to experiments with magnetic materials (nickel) where the deviation to theory amounts to a few orders of magnitude [61]. An explanation for this anomaly would turn precision measurements of forces in the sub-micrometer range into tighter constraints on gravity on small scales (including extensions of the Standard Model like the ‘fifth force’ and additional dimensions) [62–64].

Heat transfer below 10 nm

Two recent experiments on heat transfer between sharp, metallized tips and a substrate, held at different temperatures, suggest a similar anomaly when compared to fluctuation electrodynamics [65,66]. The setups differ mainly in the size of the tips (radius of curvature). The group of Reddy and Meyhofer found good agreement with theoretical calculations done by the group of García-Vidal and Cuevas [65], within uncertainties related to surface roughness. Distances down to a few nanometers were reached (tip radius ≈ 450 nm). The group of Kittel observed a heat flux much larger than theory (computed by Biehs and Rodriguez) [66], using a sharper tip (radius ≈ 30 nm) in a similar range of distances. The data show an onset of the ‘giant heat flux’ at $d \approx 5 \dots 6$ nm, with a roughly linear increase as d is reduced. According to calculations, a significant fraction of the heat flux should originate from the ‘shaft’ of the tip (conical shape with ~ 300 nm height). It has been checked that the difference between experiment and theory is not reduced when a nonlocal conductivity (spatial dispersion) is applied [66]. The solution to this anomaly in short-range heat transfer is currently under investigation [67,68]. Molecular dynamics simulations like those performed by the Volz [69] and Chen groups [70] are likely to provide a versatile tool to ‘bridge the gap’ between the mesoscopic and microscopic scales and include, for example, heat transport from phonons [71].

Conclusion

We hope that the present introduction to fluctuation electrodynamics provides a convenient ‘entry point’ into this powerful method. As it happens with any other

physical theory, it must be used having its limitations in mind. Some of these are quite natural and related to convenient approximations like a local response. The limits set by experiments that give different results, are pointing towards new challenges and may open up directions for further development.

Acknowledgments I thank the *Deutsche Forschungsgemeinschaft* for support through the DIP program (grant number FO-703/2-1).

- [1] Rytov S M, Kravtsov Y A and Tatarskii V I 1989 *Elements of Random Fields (Principles of Statistical Radiophysics vol 3)* (Berlin: Springer)
- [2] Ginsburg W L 1953 *Fortschr. Phys.* **1** 51–87 [*Uspekhi Fiz. Nauk* 46 (1952) 348–87]
- [3] Dzyaloshinskii I E, Lifshitz E M and Pitaevskii L P 1961 *Sov. Physics Usp.* **4** 153–76
- [4] Lifshitz E M and Pitaevskii L P 1980 *Statistical Physics (Part 2)* 2nd ed (Landau and Lifshitz, *Course of Theoretical Physics* vol 9) (Oxford: Pergamon)
- [5] Ben-Abdallah P and Biehs S A 2015 *AIP Adv.* **5** 053502
- [6] Song B, Fiorino A, Meyhofer E and Reddy P 2015 *AIP Advances* **5** 053503
- [7] Liu X, Wang L and Zhang Z M 2015 *Nanoscale Microscale Thermophys. Eng.* **19** 98–126
- [8] Jones A C, O’Callahan B T, Yang H U and Raschke M B 2013 *Progr. Surf. Sci.* **88** 349–92
- [9] Dorofeyev I A and Vinogradov E A 2011 *Phys. Rep.* **504** 75–143
- [10] Narayanaswamy A, Shen S, Hu L, Chen X and Chen G 2009 *Appl. Phys. A* **96** 357–62
- [11] Greffet J J and Henkel C 2007 *Contemp. Phys.* **48** 183–94
- [12] Henkel C 2006 *Nanometer-scale electromagnetic field fluctuations in Handbook of Theoretical and Computational Nanotechnology*, edited by Rieth M and Schommers W (Stevenson Ranch, California: American Scientific Publishers) vol 7, chap 25, pp 463–501
- [13] Henry C H and Kazarinov R F 1996 *Rev. Mod. Phys.* **68** 801
- [14] Einstein A 1905 *Ann. Phys. (Leipzig)* **322** 549–60, former citation: *Ann. d. Physik, Vierte Folge* **17**, 549–60
- [15] García-Moliner F and Flores F 1979 *Introduction to the theory of solid surfaces* (Cambridge and London: Cambridge University Press)
- [16] Bedeaux D and Vlieger J 2004 *Optical Properties of Surfaces* (Singapore: World Scientific)
- [17] Liebsch A 1993 *Phys. Rev. Lett.* **71** 145–48 comment: P. J. Feibelman 1994 *Phys Rev Lett* **72** 788 & reply p 789
- [18] Asger Mortensen N, Raza S, Wubs M, Søndergaard T and Bozhevolnyi S I 2014 *Nature Commun.* **5** 3809
- [19] Buhmann S Y, Butcher D T and Scheel S 2012 *New J. Phys.* **14** 083034
- [20] Pitaevskii L P 2009 *Las. Phys.* **19** 632–35 (Preprint [arXiv:0905.3493](https://arxiv.org/abs/0905.3493))
- [21] Barash Y S and Ginzburg V L 1975 *Sov. Phys. Usp.* **18** 305–22
- [22] Scheel S and Welsch D G 2006 *Phys. Rev. Lett.* **96** 073601
- [23] Soo H and Krüger M 2016 *Europhys. Lett.* In press (Preprint [arXiv:1604.05568](https://arxiv.org/abs/1604.05568))
- [24] Xu J B, Lauger K, Moller R, Dransfeld K and Wilson I H 1994 *J. Appl. Phys.* **76** 7209–16
- [25] Shayduk R, Navirian H, Leitenberger W, Goldshteyn J, Vrejoiu I, Weinelt M, Gaal P, Herzog M, von Korff Schmising C and Bargheer M 2011 *New J. Phys.* **13** 093032

- [26] Callen H B and Welton T A 1951 *Phys. Rev.* **83** 34–40
- [27] Usami K, Nambu Y, Shi B S, Tomita A and Nakamura K 2004 *Phys. Rev. Lett.* **92** 113601
- [28] Di Stefano O, Savasta S and Girlanda R 2000 *Phys. Rev. A* **61** 02 3803
- [29] Knöll L, Scheel S and Welsch D G 2001 *QED in dispersing and absorbing dielectric media* in *Coherence and Statistics of Photons and Atoms*, edited by J. Peřina (New York: John Wiley & Sons, Inc.) chap 1, pp 1–64 (Preprint quant-ph/0006121)
- [30] Jackson J D 1975 *Classical Electrodynamics* 2nd ed (New York: Wiley & Sons)
- [31] Wylie J M and Sipe J E 1984 *Phys. Rev. A* **30** 1185–93
- [32] Sipe J E 1987 *J. Opt. Soc. Am. B* **4** 481–89
- [33] Tomař M S 1995 *Phys. Rev. A* **51** 2545–59
- [34] Chew H 1987 *J. Chem. Phys.* **87** 1355–60
- [35] Parsegian V A 2006 *Van der Waals Forces – A Handbook for Biologists, Chemists, Engineers, and Physicists* (New York: Cambridge University Press)
- [36] Chew W C 1999 *Waves and Fields in Inhomogeneous Media* Electromagnetic Waves (Wiley-IEEE Press)
- [37] Levin M and Rytov S 1974 *Sov. Phys. JETP* **38** 688–92 [*ZhETF* **65**(4), 1382–91 (1974)]
- [38] Reid M T H, Rodriguez A W and Johnson S G 2013 *Proc. IEEE* **101** 531–45
- [39] Rodriguez A, Ibanescu M, Iannuzzi D, Capasso F, Joannopoulos J D and Johnson S G 2007 *Phys. Rev. Lett.* **99** 080401
- [40] Lifshitz E M 1956 *Soviet Phys. JETP* **2** 73–83 [*J. Exper. Theoret. Phys. USSR* **29**, 94 (1955)]
- [41] Buhmann S Y 2012 *Dispersion Forces I – Macroscopic Quantum Electrodynamics and Ground-State Casimir, Casimir-Polder and van der Waals Forces* (*Springer Tracts in Modern Physics* vol 247) (Heidelberg: Springer)
- [42] Eckhardt W 1984 *Phys. Rev. A* **29** 1991–2003
- [43] Scheel S, Knöll L and Welsch D G 1998 *Phys. Rev. A* **58** 700–706
- [44] Agarwal G S 1975 *Phys. Rev. A* **11** 230–42
- [45] Barton G 2015 *J. Phys. Condens. Matt.* **27** 214005
- [46] Barton G 2016 *J. Stat. Phys.* Submitted
- [47] Loomis J J and Maris H J 1994 *Phys. Rev. B* **50** 18517–24
- [48] Chandrasekhar S 1960 *Radiative Transfer* (New York: Dover)
- [49] Setälä T, Kaivola M and Friberg A T 2002 *Phys. Rev. Lett.* **88** 123902
- [50] Ellis J, Dogariu A, Ponomarenko S and Wolf E 2005 *Opt. Commun.* **248** 333–37
- [51] Agarwal G S, Gbur G and Wolf E 2004 *Opt. Lett.* **29** 459–61
- [52] Zurita-Sánchez J R 2016 *J. Opt. Soc. Am. A* **33** 118–30
- [53] Babuty A, Joulain K, Chapuis P O, Greffet J J and De Wilde Y 2013 *Phys. Rev. Lett.* **110** 146103
- [54] Li X L, Ford G W and O’Connell R F 1993 *Phys. Rev. E* **48** 1547–49 comment: Senitzky, *Phys Rev E* **51** (1995) 5166; reply: *Phys Rev E* **51** (1995) 5169
- [55] Polder D and van Hove M 1971 *Phys. Rev. B* **4** 3303–14
- [56] Dalvit D A R, Milonni P W, Roberts D and da Rosa F (eds) 2011 *Casimir physics* (*Lecture Notes in Physics* vol 834) (Berlin Heidelberg: Springer)
- [57] Simpson W and Leonhardt U (eds) 2015 *Forces of the Quantum Vacuum – An Introduction to Casimir Physics* (Singapore: World Scientific)
- [58] Chen F, Klimchitskaya G L, Mostepanenko V M and Mohideen U 2007 *Opt. Express* **15** 4823–29

- [59] Chen F, Klimchitskaya G L, Mostepanenko V M and Mohideen U 2007 *Phys. Rev. B* **76** 035338
- [60] Svetovoy V B 2008 *Phys. Rev. Lett.* **101** 163603 erratum: *Phys. Rev. Lett.* **102** (2009) 219903
- [61] Bimonte G, Lopez D and Decca R S 2016 *Phys. Rev. B* **93** 184434
- [62] Decca R S, Lopez D, Fischbach E, Klimchitskaya G L, Krause D E and Mostepanenko V M 2007 *Phys. Rev. D* **75** 077101
- [63] Decca R, López D, Fischbach E, Klimchitskaya G, Krause D and Mostepanenko V 2007 *Eur. Phys. J. C* **51** 963–75
- [64] Chen Y J, Tham W K, Krause D E, Lopez D, Fischbach E and Decca R S 2016 *Phys. Rev. Lett.* **116** 221102 (*Preprint arXiv:1410.7267*)
- [65] Kim K, Song B, Fernández-Hurtado V, Lee W, Jeong W, Cui L, Thompson D, Feist J, Reid M T H, García-Vidal F J, Cuevas J C, Meyhofer E and Reddy P 2015 *Nature* **528** 387–91
- [66] Kloppstech K, Könné N, Biehs S A, Rodriguez A W, Worbes L, Hellmann D and Kittel A 2015 Giant near-field mediated heat flux at the nanometer scale (*Preprint arXiv:1510.06311*)
- [67] Wang S, Ng J, Xiao M and Chan C T 2016 *Science Adv.* **2** e1501485 (*Preprint arXiv:1510.06227*)
- [68] Wang J S and Peng J 2016 A microscopic theory for ultra-near-field radiation (*Preprint arXiv:1607.02840*)
- [69] Domingues G, Volz S, Joulain K and Greffet J J 2005 *Phys. Rev. Lett.* **94** 085901
- [70] Chiloyan V, Garg J, Esfarjani K and Chen G 2015 *Nature Commun.* **6** 6755
- [71] Mingo N 2009 *Green's Function Methods for Phonon Transport Through Nano-Contacts in Thermal Nanosystems and Nanomaterials*, edited by S. Volz (*Topics in Applied Physics* vol 118) (Springer) chap 3, pp 63–94